THE STIFF LIMIT OF THE EXPONENTIAL ROSENBROCK-TYPE METHOD

Michelle Hine
May 26, 2011

ABSTRACT

In this paper, I explore the exponential Rosenbrock-type method of order two. It is an explicit method that solves stiff ODEs. The method linearizes the equation with each step, then uses a matrix exponential to solve the linearized equation exactly. Previous research has identified stability bounds and convergence results. In this paper, I explore the stiffness capabilities of this second order method as stiffness increases toward infinity. The paper contains estimation-style analysis of the step size and order. I also test the exponential Rosenbrock-type method on two stiff equations: decay of a particle to a circle, and a partial differential equation on a circle with either a viscosity or a hyperviscosity term. Through numerical testing, it is evident that the exponential Rosenbrock-type method exhibits stiffness characteristics in the limit as stiffness tends towards infinity; however, for high stiffness, the method has order reduction to first order.

1. INTRODUCTION

1.1. **Stiff Problems.** An ordinary differential equation is considered stiff if it has widely fluctuating time scales, i.e., it contains a mode that is rapidly decaying on the scale of the whole problem [2]. For problems with both rapidly and slowly oscillating modes, a smaller step size is needed near the beginning of the time interval. As time increases, the rapidly oscillating modes die down, and the slower oscillating modes dominate the system. After enough time has passed, a relatively large step size is sufficient to accurately capture the behavior of the system.

To determine whether a problem has stiff decay, consider the eigenvalues of the Jacobian from the equation of motion. Systems exhibiting stiff decay can have a mixture of eigenvalues with large negative real parts and those with small negative real parts; or eigenvalues that are large and almost purely imaginary [1, 2]. The latter case results in rapidly oscillating problems with slow decay.

1.2. **Comparison with Standard Methods.** Typically, one uses implicit methods to handle problems with stiff decay. The goal of this research is to explore an explicit solver that properly handles stiff problems. Standard methods for solving differential equations, such as Runge Kutta or linear multistep, are inappropriate here because these traditional methods are either implicit or do not possess stiff decay properties.

This paper does not focus on computational efficiency. This research is not meant to create an industrial quality code, but merely explore the stiffness capabilities of the exponential Rosenbrock-type integrator. In the spirit of preliminary research, calculations are simplified by working with autonomous equations.

1.3. **Introduction to the Exponential Rosenbrock-type Method.** To solve a differential equation, the exponential Rosenbrock-type integrator linearizes the equation, then solves the linear equation exactly. Exponential integrators are not a new method; the first prototypes appeared nearly 50 years ago [4]. Historically, most exponential-style integrators linearized the equation only at the initial time step. More recently, people began to linearize the problem with each time step, resulting in a much more accurate solution curve. Exponential Rosenbrock-type methods of different orders exist; in 2009, Hockbruck, *et al.* introduced multistage methods of orders three and four [4]. I focus on the single-stage method of second order.

The exponential Rosenbrock-type method of order two is an explicit one-step method, so the next step only depends on the current values of the system. With each step, the method linearizes the equation using the Jacobian matrix:

$$\begin{aligned} \mathbf{y}' &= f(\mathbf{y}) \\ &\approx f(\mathbf{y}_{k-1}) + \tfrac{df}{d\mathbf{y}}\big|_{\mathbf{y}=\mathbf{y}_{k-1}}(\mathbf{y}-\mathbf{y}_{k-1}) \\ &= f(\mathbf{y}_{k-1}) + J(\mathbf{y}-\mathbf{y}_{k-1}). \end{aligned} \tag{1}$$

Using the matrix exponential, the exponential Rosenbrock-type integrator solves the linear equation exactly, and then steps forward by the exact solution of the linear equation. A more explicit derivation of the method follows in a latter section of the paper. For each time step, the solution obtained is

$$\mathbf{y}(t) = e^{(t-t_{k-1})J}\mathbf{y}_{k-1} + \int_{t_{k-1}}^{t} e^{(t-\tau)J}\big(f(\mathbf{y}_{k-1}) - J\mathbf{y}_{k-1}\big)d\tau. \tag{2}$$

Assuming the inverse Jacobian exists, the solution can be rewritten as

$$\mathbf{y}(t) = \mathbf{y}_{k-1} + \big(e^{(t-t_{k-1})J} - I\big)J^{-1}f(\mathbf{y}_{k-1}). \tag{3}$$

I used this equivalent solution to the linearized equation in the numerical tests studied for this paper.

2. Testing of Stiff Decay

2.1. **Standard Methods to Test Stiff Decay.** The standard test described by Ascher and Petzold to determine whether a given method handles stiff decay is to analyze a slightly generalized test equation, including an inhomogeneity [1]. One considers the test equation

$$y' = \lambda(y - g(t)), \tag{4}$$

with $g(t)$ a bounded, but arbitrary function. The method has stiff decay if for a fixed $t_n > 0$, the function behavior decays to the inhomogeneity, i.e., $|y_n - g(t_n)| \to 0$ as $h_n Re(\lambda) \to -\infty$.

Consider an equation with both slow and fast modes. As time increases, the fast modes decay leaving behind only the slow modes, $g(t)$. In the test equation, the function $g(t)$ represents slow modes that continue to affect the behavior of the system as $t \to \infty$.

For the exponential Rosenbrock-type method considered in this paper, Ascher and Petzold's stiffness criterion is automatically satisfied because equation (4) is linear in terms of y. Consider testing the exponential Rosenbrock-type method with the autonomous equation $\mathbf{y}' = \lambda y$. For $z = h\lambda$, the amplification function is $R(z) = e^z$, so the method solves the system exactly. Hence, Ascher and Petzold's approach to determining stiff decay is useless here, since the stiff decay criterion for the linear autonomous equation is trivially satisfied. Instead, I test the method on equations with stiff decay. This is not a new idea; other authors have also used test problems to explore the stiffness of methods [2, 3, 4].

To achieve stiff decay, I use test equations containing both fast and slow modes. This is similar in spirit to the test equation with an inhomogeneity.

2.2. **Test Equations.** Two main test cases are considered: decay to a circle and partial differential equations with viscosity or hyperviscosity on a circle. For the first case, consider a particle with some initial position. It decays to a circle, and then continues rotating around the circle. The motion of the particle is described by equation (5), where the dot denotes derivative in time.

$$\begin{cases} \dot{x} = -y - \lambda x(x^2+y^2-1) \\ \dot{y} = \quad x - \lambda y(x^2+y^2-1) \end{cases} \tag{5}$$

The decay to the circle provides the fast mode, then counter-clockwise rotation acts as the slow mode. The stiffness of the equation is governed directly by the parameter λ. Larger values of λ correspond with higher stiffness, and faster decay to the circle. In Figure 1, it is apparent that with $\lambda = 20$, the particle decays much more quickly to the circle than with $\lambda = 1$.

FIGURE 1. Decay to a circle, with two different values of λ.

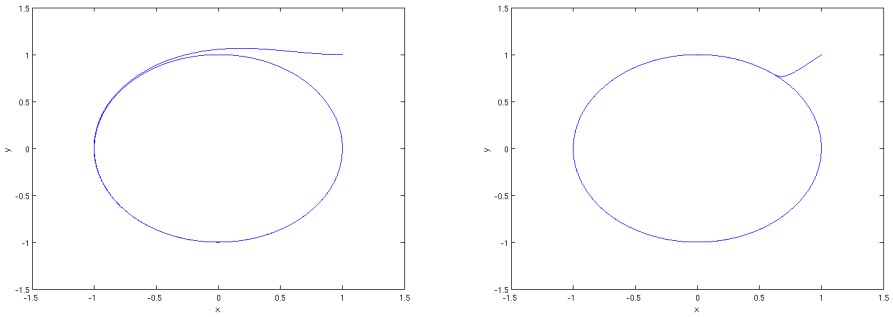

(A) $\lambda = 1$ (B) $\lambda = 20$

For the second case, consider points a circle with the diffusion equation and nonlinear forcing:

$$u_t = u_{xx} - u^3. \tag{6}$$

Finite differences are used for the derivative in x. The motion of each point u_i is described by equation (7), where the dot denotes derivative in time, and Δx is the distance between the discretized points on the circle.

$$\dot{u_i} = \frac{u_{i-1} - 2u_i + u_{i+1}}{\Delta x^2} - u_i^3 \tag{7}$$

Figure 2 shows the diffusion equation with nonlinear forcing, with initial conditions of

$$u(\theta,0) = \begin{cases} 1 & \text{if } 0 \le \theta \le \pi/2 \\ -1 & \text{if } \pi/2 \le \theta \le 3\pi/2 \\ 1 & \text{if } 3\pi/2 \le \theta \le 2\pi. \end{cases} \tag{8}$$

The system exhibits an initial period of fast decay, followed by a period of slow oscillation. Given sufficient time, the system will decay to zero.

FIGURE 2. The diffusion equation on a circle, with 400 discretized points, $t = 1.5$.

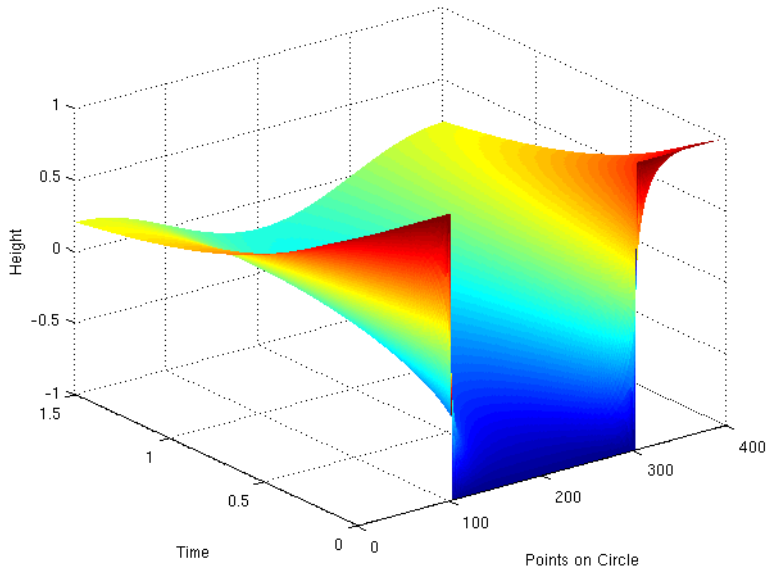

Similarly, consider points on a circle with a differential equation including a hyperviscocity term:

$$u_t = u_{xxxx} - u^3. \tag{9}$$

Again, finite differences are used for the derivative in x. Each point u_i is described by equation (10), where the dot denotes derivative in time, and Δx is the distance between the discretized points on the circle.

$$\dot{u}_i = \frac{-u_{i-2} + 4u_{i-1} - 6u_i + 4u_{i+1} - u_{i+2}}{\Delta x^4} - u_i^3 \tag{10}$$

The high frequency harmonics provide fast modes while the low frequency harmonics provide slow modes. The equation exhibits rapid decay of the fast modes, then continues on with the slow dynamics of the system. Figure 3 shows the hyperviscosity equation with nonlinear forcing, and the same initial conditions as in equation (8). Due to the hyperviscosity term, new maxima and minima are created during the initial evolution of the system behavior. The extrema die off rapidly, and then the long-term behavior of the system is governed by the slow modes. The stiffness of the problem increases with the number of points on our discretized circle.

If a method properly handles stiff decay, it will traverse the slow dynamics with a step size that is not small. The exponential Rosenbrock-type method allows the fast modes to continue to decay as the system travels through the slow dynamics. Once the system has passed through the region of rapid decay, the step size h should be prescribed by the slow dynamics of the system. In the stiff limit, the exponential Rosenbrock-type method should

FIGURE 3. The hyperviscocity equation on a circle, with 400 discretized points, $t = 1.5$.

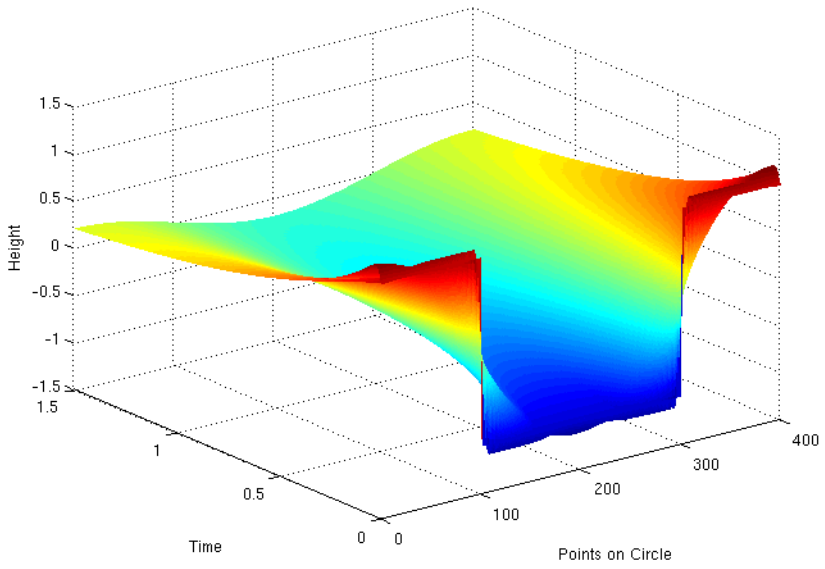

still exhibit reasonable step sizes. Ideally, the step size depends on the tolerance level set for the solver, and is not based on the stiffness of the problem.

3. DERIVATION OF THE EXPONENTIAL ROSENBROCK-TYPE METHOD

To derive the exponential Rosenbrock-type integrator, one begins with the autonomous differential equation, $\mathbf{y}' = \mathbf{f}(\mathbf{y})$. First, one linearizes about $\mathbf{y}_{k-1}$ using a Taylor expansion.

$$\mathbf{y}' = \mathbf{f}(\mathbf{y}_{k-1}) + \left.\frac{\partial \mathbf{f}}{\partial \mathbf{y}}\right|_{\mathbf{y}=\mathbf{y}_{k-1}} (\mathbf{y}-\mathbf{y}_{k-1}) = \mathbf{f}(\mathbf{y}_{k-1}) + J|_{\mathbf{y}=\mathbf{y}_{k-1}}(\mathbf{y}-\mathbf{y}_{k-1})$$

Rearrange terms to write the equation as $\mathbf{y}' = J\mathbf{y} + (\text{inhomogeneity})$.

$$\mathbf{y}' = J|_{\mathbf{y}=\mathbf{y}_{k-1}}\mathbf{y} + \left(\mathbf{f}(\mathbf{y}_{k-1}) - J|_{\mathbf{y}=\mathbf{y}_{k-1}}\mathbf{y}_{k-1}\right).$$

Solving the differential equation yields the solution curve:

$$\mathbf{y}(t) = e^{(t-t_{k-1})J}\mathbf{y}_{k-1} + \int_{t_{k-1}}^{t} e^{(t-\tau)J}\left(f(\mathbf{y}_{k-1}) - J\mathbf{y}_{k-1}\right)d\tau. \tag{11}$$

Assuming the inverse Jacobian exists, one can use J^{-1} to calculate the integral of the matrix exponential, and for $h = t - t_{k-1}$, equation (11) becomes

$$\begin{aligned}\mathbf{y}(t) &= e^{hJ}\mathbf{y}_{k-1} + (e^{hJ} - I)J^{-1}\left(f(\mathbf{y}_{k-1}) - J\mathbf{y}_{k-1}\right)\\ &= e^{hJ}\mathbf{y}_{k-1} + (e^{hJ} - I)J^{-1}f(\mathbf{y}_{k-1}) - (e^{hJ} - I)\mathbf{y}_{k-1}.\end{aligned}$$

Finally, the solution to the linearized autonomous equation can be written as

$$\mathbf{y}(t) = \mathbf{y}_{k-1} + (e^{hJ} - I)J^{-1}f(\mathbf{y}_{k-1}). \tag{12}$$

For the test problems considered in this paper, the inverse Jacobian exists. Hence, the code uses the solution to the linearized equation contained in equation (12). In the next section, I analyze the dependence of step size on tolerance level.

4. Analysis of Order in the Stiff Limit Approaching Infinity

4.1. **Analysis of Step Size Choice.** To determine analytically how step size is depends on tolerance, apply the exponential Rosenbrock-type method to the equation $\mathbf{y}' = \mathcal{F} \triangleq \lambda F + f$, where F denotes the fast decaying modes of the system, and f denotes the slow modes of the system. Note that the Jacobian is then $\mathcal{J} = \lambda J + j$. By assumption, f is not large in λ. The adaptive step method accepts a step size based on a tolerance criterion on the difference of the solutions obtained by simultaneous runs with different step sizes. To analyze step choice based on tolerance level, apply the method to both step sizes.

For simplicity, consider the method beginning at time 0 with a step size of h. Apply one step of h to obtain $\mathbf{y}_k$ and two steps of $h/2$ to obtain $\bar{\mathbf{y}}_k$.

$$\left\{ \mathbf{y}_k = \mathbf{y}_{k-1} + \int_0^h e^{\tau \mathcal{J}_{k-1}} \mathcal{F}_{k-1} d\tau \right.$$

$$\left\{ \begin{array}{rl} \mathbf{y}_{k-1/2} & = \mathbf{y}_{k-1} + \int_0^{h/2} e^{\tau \mathcal{J}_{k-1}} \mathcal{F}_{k-1} d\tau \\ \bar{\mathbf{y}}_k & = \mathbf{y}_{k-1/2} + \int_0^{h/2} e^{\tau \mathcal{J}_{k-1/2}} \mathcal{F}_{k-1/2} d\tau \end{array} \right.$$

For clarity of notation, define $\mathcal{J} \triangleq \mathcal{J}_{k-1}$, $\mathcal{F} \triangleq \mathcal{F}_{k-1}$, $\tilde{\mathcal{J}} \triangleq \mathcal{J}_{k-1/2}$, and $\tilde{\mathcal{F}} \triangleq \mathcal{F}_{k-1/2}$. Since $\mathcal{F}$ and $\tilde{\mathcal{F}}$ do not depend on τ, they may be factored out of the integral. Combining the last two lines yields the solution obtained by two applications of step size $h/2$:

$$\bar{\mathbf{y}}_k = \mathbf{y}_{k-1} + \left(\int_0^{h/2} e^{\tau \mathcal{J}} d\tau \right) \mathcal{F} + \left(\int_0^{h/2} e^{\tau \tilde{\mathcal{J}}} d\tau \right) \tilde{\mathcal{F}}.$$

Then subtracting the two methods yields equation (13).

$$\begin{aligned} \mathbf{y}_k - \bar{\mathbf{y}}_k = & \left[\mathbf{y}_{k-1} + \left(\textstyle\int_0^h e^{\tau \mathcal{J}} d\tau \right) \mathcal{F} \right] \\ & - \left[\mathbf{y}_{k-1} + \left(\textstyle\int_0^{h/2} e^{\tau \mathcal{J}} d\tau \right) \mathcal{F} + \left(\textstyle\int_0^{h/2} e^{\tau \tilde{\mathcal{J}}} d\tau \right) \tilde{\mathcal{F}} \right] \end{aligned} \tag{13}$$

One can split the first integral into two pieces, $\int_0^{h/2} e^{\tau \mathcal{J}} d\tau$ and $\int_{h/2}^h e^{\tau \mathcal{J}} d\tau$. Then consider the Taylor expansion of $\tilde{\mathcal{F}}$, where the ellipses represent the nonlinear terms.

$$\begin{aligned} \tilde{\mathcal{F}} &= \mathcal{F} \left(\mathbf{y}_{k-1} + \left(\textstyle\int_0^{h/2} e^{\tau \mathcal{J}} d\tau \right) \mathcal{F} \right) \\ &= \mathcal{F} + \mathcal{J} \left(\textstyle\int_0^{h/2} e^{\tau \mathcal{J}} \right) \mathcal{F} + \ldots \\ &= \left[I + \mathcal{J} \left(\textstyle\int_0^{h/2} e^{\tau \mathcal{J}} \right) \right] \mathcal{F} + \ldots \end{aligned}$$

One can show that that $I + \mathcal{J} \left(\int_0^{h/2} e^{\tau \mathcal{J}} \right) = e^{\frac{h}{2} \mathcal{J}}$. Using this identity and solving for the nonlinear terms allows the expression for $\tilde{\mathcal{F}}$ to be rewritten as

$$\tilde{\mathcal{F}} = e^{\frac{h}{2} \mathcal{J}} \mathcal{F} + \left(\tilde{\mathcal{F}} - e^{\frac{h}{2} \mathcal{J}} \mathcal{F} \right), \tag{14}$$

where $\tilde{\mathcal{F}} - e^{\frac{h}{2}\mathcal{J}}\mathcal{F}$ represents the nonlinear terms. After cancellation and substituting in the linearization of $\tilde{\mathcal{F}}$, equation (13) becomes

$$\begin{aligned}
&= \int_{h/2}^{h} e^{\tau\mathcal{J}}\mathcal{F}\,d\tau - \int_0^{h/2} e^{\tau\tilde{\mathcal{J}}}\tilde{\mathcal{F}}\,d\tau \\
&= \int_{h/2}^{h} e^{\tau\mathcal{J}}\mathcal{F}\,d\tau - \int_0^{h/2} e^{\tau\tilde{\mathcal{J}}}\left(e^{\frac{h}{2}\mathcal{J}}\mathcal{F} + \left(\tilde{\mathcal{F}} - e^{\frac{h}{2}\mathcal{J}}\mathcal{F}\right)\right)d\tau \\
&= \left[\int_{h/2}^{h} e^{\tau\mathcal{J}}d\tau - \int_0^{h/2} e^{\tau\tilde{\mathcal{J}}}e^{\frac{h}{2}\mathcal{J}}d\tau\right]\mathcal{F} + \int_0^{h/2} e^{\tau\tilde{\mathcal{J}}}\left(e^{\frac{h}{2}\mathcal{J}}\mathcal{F} - \tilde{\mathcal{F}}\right)d\tau.
\end{aligned}$$

Adjusting the limits of integration of the first integral and simplifying yields the expression

$$= \left[\int_{h/2}^{h} e^{(\tau-\frac{h}{2})\mathcal{J}+\frac{h}{2}\mathcal{J}}d\tau - \int_0^{h/2} e^{\tau\tilde{\mathcal{J}}}d\tau\left(e^{\frac{h}{2}\mathcal{J}}\right)\right]\mathcal{F} + \int_0^{h/2} e^{\tau\tilde{\mathcal{J}}}\left(e^{\frac{h}{2}\mathcal{J}}\mathcal{F} - \tilde{\mathcal{F}}\right)d\tau.$$

Finally, the method bounds the difference $|\mathbf{y}-\bar{\mathbf{y}}|$ by the tolerance level, TOL.

$$|\mathbf{y}-\bar{\mathbf{y}}| = \left|\left[\int_0^{h/2}\left(e^{\tau\mathcal{J}} - e^{\tau\tilde{\mathcal{J}}}\right)d\tau\right]e^{\frac{h}{2}\mathcal{J}}\mathcal{F} + \left[\int_0^{h/2} e^{\tau\tilde{\mathcal{J}}}d\tau\right]\left(e^{\frac{h}{2}\mathcal{J}}\mathcal{F} - \tilde{\mathcal{F}}\right)\right| \leq \text{TOL} \tag{15}$$

There are two main sources of difference between the methods used to obtain $\mathbf{y}$ and $\bar{\mathbf{y}}$: the difference in the exponential terms due to rotation of the Jacobian matrix, and the nonlinear terms of the expansion for $\tilde{\mathcal{F}}$. In the linear case, $\tilde{\mathcal{F}}$ exactly equals $e^{\frac{h}{2}\mathcal{J}}\mathcal{F}$. For the purposes of this analysis, I assume the nonlinear terms in the expansion are small, so the second term of the expression can be neglected. Then the difference becomes

$$|\mathbf{y}-\bar{\mathbf{y}}| = \left|\int_0^{h/2}\left(e^{\tau\mathcal{J}} - e^{\tau\tilde{\mathcal{J}}}\right)d\tau\; e^{\frac{h}{2}\mathcal{J}}\mathcal{F}\right| \leq \text{TOL}. \tag{16}$$

Consider the case where the solution has already decayed to the slow modes. Then by assumption, $\mathcal{F}$ is not large in λ. Also, $e^{\frac{h}{2}\mathcal{J}}$ is not large, because as I will argue below, it acts a projector to the slow dynamics, and the eigenvalues of $\mathcal{J}$ are mostly large and negative. Then the main difference in the two methods is caused by the change in the direction of the two projectors, $e^{\tau\mathcal{J}}$ and $e^{\tau\tilde{\mathcal{J}}}$.

4.2. **Analysis of Decay to the Stable Manifold.** Consider the same equation, $\mathbf{y}' = \mathcal{F}(\mathbf{y}) \triangleq \lambda\mathbf{F}(\mathbf{y}) + \mathbf{f}(\mathbf{y})$. I use estimation style analysis to evaluate behavior in the limit $\lambda \to \infty$.

With a large value of λ, one expects fast decay to the stable manifold $\mathbf{F}(\mathbf{y}) = \mathbf{0}$. Henceforth when the term manifold is used, it refers to the stable manifold. Let the dimension of this surface be m, and the dimension of the whole space $\mathbf{y}$ be M. Write $\mathbf{y}$ as $\mathbf{y} = \mathbf{y}_{\text{fast}} + \mathbf{y}_{\text{slow}}$, where $\mathbf{y}_{\text{fast}}$ corresponds to the fast decay part of the evolution, and $\mathbf{y}_{\text{slow}}$ represents the slow evolution of the system after the decay occurs.

Of course, $\mathbf{y}' = (\mathbf{y}_{\text{fast}} + \mathbf{y}_{\text{slow}})' = \mathcal{F}(\mathbf{y}_{\text{fast}} + \mathbf{y}_{\text{slow}})$. But this yields only M equations for $2M$ variables. One can choose M other conditions on $\mathbf{y}_{\text{fast}}$ and $\mathbf{y}_{\text{slow}}$ as one sees fit, so here I choose them according to the intuitive meaning of $\mathbf{y}_{\text{fast}}$ and $\mathbf{y}_{\text{slow}}$. Since the manifold contains the slow dynamics, $\mathbf{F}(\mathbf{y}_{\text{slow}}) = \mathbf{0}$. This yields $M-m$ additional conditions, but the system still needs m conditions. Consider distributing $\mathbf{y}$ into $\mathbf{y}_{\text{fast}}$ and $\mathbf{y}_{\text{slow}}$. One way is to choose $\mathbf{y}_{\text{slow}}$ as the closest point on the surface $\mathbf{F}(\mathbf{y}) = \mathbf{0}$. This defines an "algorithm" of finding $\mathbf{y}_{\text{fast}}$ and $\mathbf{y}_{\text{slow}}$ given $\mathbf{y}$, so it yields the remaining m conditions.

Consider a point $\mathbf{y}_{\text{slow}}$ on the surface $\mathbf{F}(\mathbf{y}) = \mathbf{0}$. One can write the orthogonal projector matrix to the plane tangent to the surface at $\mathbf{y}_{\text{slow}}$ as $\hat{P}_{\text{slow}}$. (Here, only the orientation of the plane matters, not how it is shifted from the origin). Denote the complimentary projector as

FIGURE 4. Choosing the point $\mathbf{y}_{\text{slow}}$, the closest point on the surface $\mathbf{F}(\mathbf{y}) = \mathbf{0}$, the slow dynamics of the system.

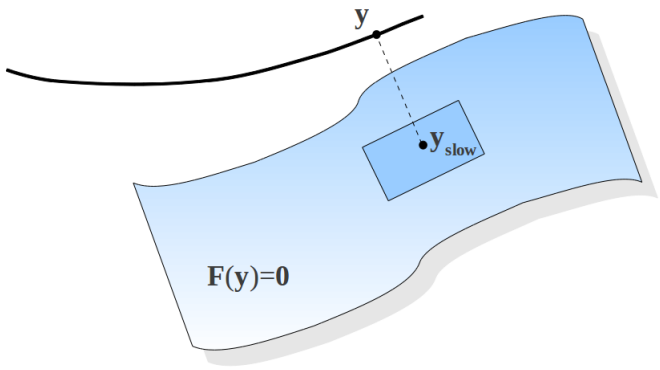

$\hat{P}_{\text{fast}}$. The remaining conditions now are written as $\hat{P}_{\text{slow}}\mathbf{y}_{\text{fast}} = \mathbf{0}$. This yields m additional conditions because only m singular values of $\hat{P}_{\text{slow}}$ are non-zero.

Let $\hat{J} = \frac{\partial \mathbf{F}}{\partial \mathbf{y}}$. The structure of $\hat{J}$ determines the projectors $\hat{P}_{\text{slow}}$ and $\hat{P}_{\text{fast}} = \hat{I} - \hat{P}_{\text{slow}}$. Namely, $\hat{P}_{\text{slow}}$ is a maximal rank (rank m) matrix such that $\hat{J}\hat{P}_{\text{slow}} = \hat{O}$, and $\hat{P}^2_{\text{slow}} = \hat{P}_{\text{slow}}$, i.e., $\hat{P}_{\text{slow}}$ is a projector.

Differentiating $\mathbf{F}(\mathbf{y}_{\text{slow}}) = \mathbf{0}$, one obtains $(\mathbf{F}(\mathbf{y}_{\text{slow}}))' = \hat{J}(\mathbf{y}_{\text{slow}})\,\mathbf{y}'_{\text{slow}} = \mathbf{0}$. Also, since $\mathbf{y}_{\text{slow}}$ is already in the slow dynamics of the system, $\hat{P}_{\text{slow}}$ projects $\mathbf{y}'_{\text{slow}}$ to itself. Then one has that $\hat{P}_{\text{fast}}\mathbf{y}'_{\text{slow}} = (I - \hat{P}_{\text{slow}})\mathbf{y}'_{\text{slow}} = \mathbf{0}$. The system of equations is then the following:

$$
\begin{aligned}
&(\mathbf{y}_{\text{fast}} + \mathbf{y}_{\text{slow}})' = \lambda \mathbf{F}(\mathbf{y}_{\text{fast}} + \mathbf{y}_{\text{slow}}) + \mathbf{f}(\mathbf{y}_{\text{fast}} + \mathbf{y}_{\text{slow}});\\
&\mathbf{F}(\mathbf{y}_{\text{slow}}) = \mathbf{0}, \quad \Rightarrow \quad \hat{J}(\mathbf{y}_{\text{slow}})\,\mathbf{y}'_{\text{slow}} = \mathbf{0} \quad \text{or} \quad \hat{P}_{\text{fast}}\mathbf{y}'_{\text{slow}} = \mathbf{0};\\
&\hat{P}_{\text{slow}}\mathbf{y}_{\text{fast}} = \mathbf{0}.
\end{aligned}
\tag{17}
$$

One can then use adiabatic approximation on the system. Here just the leading order is shown. One neglects $\mathbf{y}'_{\text{fast}}$—it is small because the solution is close to the stable manifold. One expects $\mathbf{y}_{\text{fast}} \sim 1/\lambda$, so expanding $\mathbf{F}(\mathbf{y})$ about $\mathbf{y}_{\text{slow}}$ yields $\mathbf{F}(\mathbf{y}) = \big(\mathbf{F}(\mathbf{y}_{\text{slow}}) = \mathbf{0}\big) + \hat{J}(\mathbf{y}_{\text{slow}})\mathbf{y}_{\text{fast}} + \mathrm{O}(1/\lambda^2)$. Then in equation (17), the leading order is

$$\mathbf{y}'_{\text{slow}} = \lambda \hat{J}(\mathbf{y}_{\text{slow}})\mathbf{y}_{\text{fast}} + \mathbf{f}(\mathbf{y}_{\text{slow}})$$

Acting on the system with the fast projector, $\hat{P}_{\text{fast}}$, projects the system onto the region of fast decay:

$$\lambda \hat{P}_{\text{fast}}\hat{J}(\mathbf{y}_{\text{slow}})\mathbf{y}_{\text{fast}} = -\hat{P}_{\text{fast}}\mathbf{f}(\mathbf{y}_{\text{slow}})$$

This equation can be solved for $\mathbf{y}_{\text{fast}}$. One can think of this system as a non-singular square system in the subspace related to $\hat{P}_{\text{fast}}$. It is a nondegenerate system because when considered in the $\hat{P}_{\text{fast}}$ subspace, the system decays in all directions. Note that in $1/\lambda$ order, the magnitude of $\mathbf{y}_{\text{fast}}$ is determined by $\hat{P}_{\text{fast}}\mathbf{f}$. Hence, $\mathbf{y}_{\text{fast}}$ is $\mathrm{O}(1/\lambda)$ distance from the manifold.

Thus, after the system has decayed, the solution curve is at a distance of $\mathrm{O}(1/\lambda)$. Consider the system $\mathbf{y}' = \mathcal{F} \triangleq \lambda F + f$, and project $\mathbf{y}$ onto the closest point in the manifold, $\mathbf{y}_{\text{slow}}$. Let J_* be the Jacobian at the projected point $\mathbf{y}_{\text{slow}}$. Then the Jacobian $\mathcal{J} = \lambda J + j$, so it can be rewritten as $\mathcal{J} = \lambda(J - J_*) + \lambda J_* + j$. By assumption, j represents the slow dynamics of the system, so not much change is possible in a single time step. Then

$\tau j = \mathrm{O}(h)$, since $\tau = \mathrm{O}(h)$. As before, the solution has essentially decayed to the manifold, so $\mathbf{y} - \mathbf{y}_{\text{slow}} = \mathrm{O}\left(\frac{1}{\lambda}\right)$, and then also $J - J_* = \mathrm{O}\left(\frac{1}{\lambda}\right)$. Then one can rewrite

$$\begin{aligned} e^{\tau \mathcal{J}} &= e^{\tau(\lambda J + j)} \\ &= e^{\tau[\lambda(J - J_*) + \lambda J_* + j]} \\ &= e^{\tau \lambda J_* + \mathrm{O}(h)}, \end{aligned}$$

where $\mathrm{O}(h)$ is from $\lambda(J - J_*)$ and from j. So this is a projector onto the slow dynamics, up to exponentially small terms, which are neglected. Similarly, $e^{\tau \tilde{\mathcal{J}}} = e^{\tau \lambda \tilde{J}_* + \mathrm{O}(h)}$. Hence, both $e^{\tau \mathcal{J}}$ and $e^{\tau \tilde{\mathcal{J}}}$ are projectors onto the stable manifold, up to exponentially small terms.

Then $e^{\tau \mathcal{J}} - e^{\tau \tilde{\mathcal{J}}} = \mathrm{O}(h)$, where the $\mathrm{O}(h)$ is from the difference between the projectors, due to the change in position from $\mathbf{y}_{k-1/2}$ to $\mathbf{y}_k$. The two projectors are the identical up to $\mathrm{O}(h)$ since the manifold contains the the slow dynamics of the system, and hence, $\mathcal{J}$ changes very slowly. Consider equation (16), rewritten below:

$$|\mathbf{y} - \bar{\mathbf{y}}| = \left| \int_0^{h/2} \left(e^{\tau \mathcal{J}} - e^{\tau \tilde{\mathcal{J}}} \right) d\tau \; e^{\frac{h}{2} \mathcal{J}} \mathcal{F} \right| \leq \mathrm{TOL}.$$

One obtains $\mathrm{O}(\mathrm{h})$ from the integration, and another $\mathrm{O}(\mathrm{h})$ from the difference between the two projectors. One has that $e^{\frac{h}{2} \mathcal{J}}$ is $\mathrm{O}(1)$, since it acts a projector to the slow dynamics, and the eigenvalues of $\mathcal{J}$ are mostly large and negative. Also, by assumption, $\mathcal{F}$ is not large in λ. Then the local error is $\mathrm{O}(h^2)$, which corresponds with a first order method. Hence, in the stiff limit, the method suffers from an order reduction due to the rapid change allowed between the two projector matrices.

FIGURE 5. Decay to a circle, with λ vs. number of step evaluations, $t = 3$

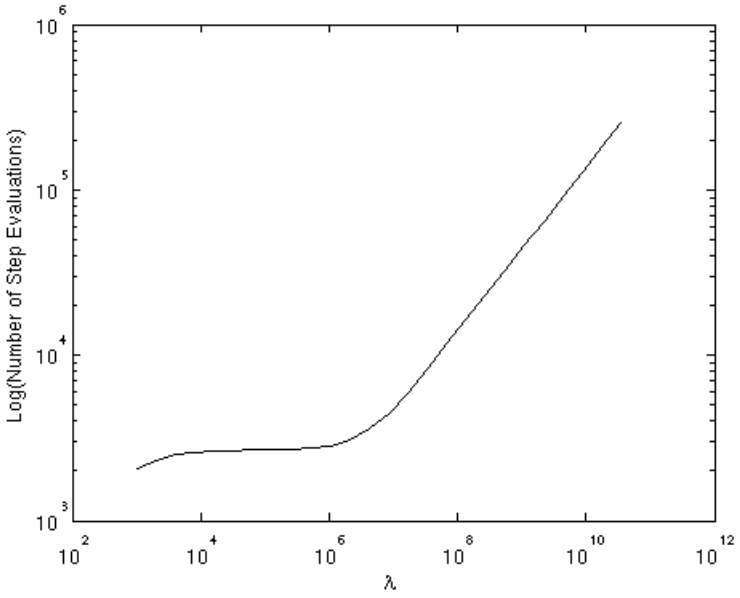

5. NUMERICAL RESULTS

5.1. **Numerical Testing of Stiff Decay Properties.** To examine whether the exponential Rosenbrock-type method exhibits stiff decay properties, numerical testing on the two example problems is used. Recall the first test problem, decay to a circle as described in equation (5). Stiffness increases directly with an increasing λ parameter. To determine how the step size of the method behaves, I ran the method with an adaptive step size. The code ran two simultaneous versions of the exponential Rosenbrock-type integrator, one with half the step size of the other. The code use forced the two versions to converge to within some tolerance before a step size was accepted. The code also allowed growth in step size for when convergence was achieved to well within the tolerance level.

Note that in Figure 5, there is a period of non-changing step size for λ values between 10^4 and 10^6. This period of constant step size indicates that the method exhibits stiff decay characteristics, but the increase after $\lambda = 10^6$ is troubling.

Substituting an alternate method for the calculation of the integral did not change the output, so it seems the increase in step size is not related to rounding errors due to the integration of the matrix exponential. Similarly, converting to single precision did not significantly alter the period of non-changing step size.

To check the behavior of step size after the solution has decayed to a circle, I ran the exponential Rosenbrock-type method for sufficient time to allow decay, then computed the average step size by looking at the last 1000 steps. Plotting different tolerance levels suggests that the area of nonincreasing step size proceeds to the right for lower tolerance thresholds, as seen in Figure 6. This corresponds with the analysis that step size depends on the tolerance.

FIGURE 6. Decay to a circle, with λ vs. average step size after decay. Average step size calculated using last 1000 steps after decay to a circle; tolerance levels of $10^{-5.5}$, 10^{-6}, and 10^{-7}.

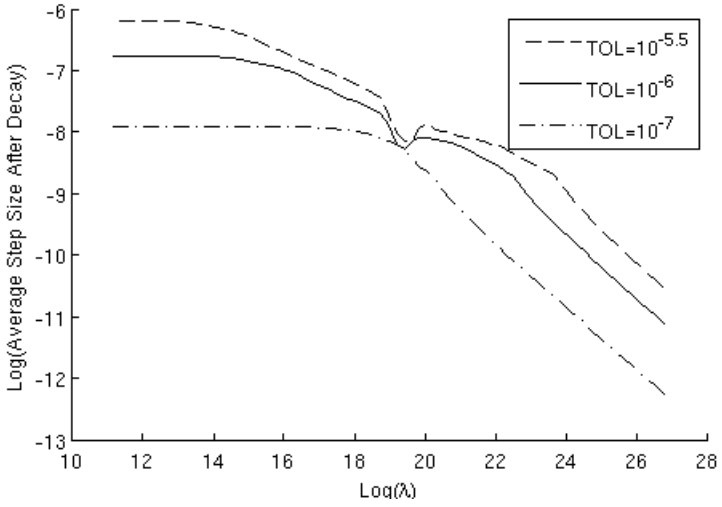

FIGURE 7. Log(Step Size) vs. Time for the equation $u_t = u_{xx} - u^3$ with N=100, N=200, and N=400; $t = 1.5$

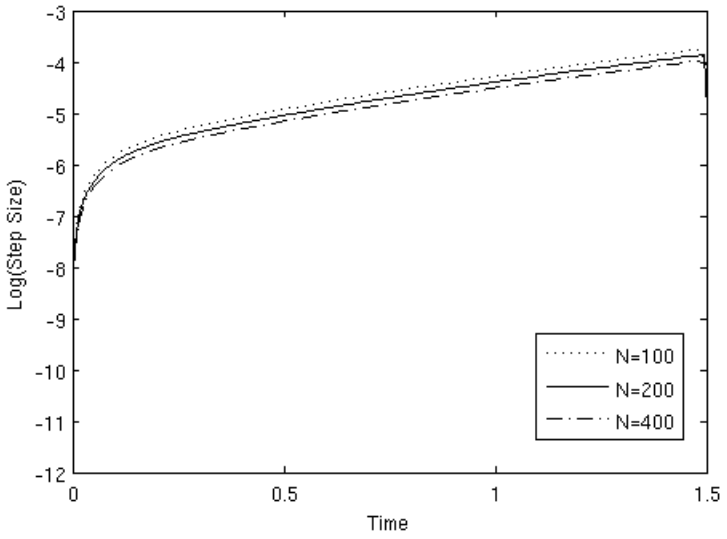

I also examined changing step sizes for the diffusion and hyperviscosity equations. Figure 7 shows that step size does grow slightly for larger numbers of discretized points; however, the growth rate is linear for the period after decay of fast modes. Again, this provides evidence of stiff decay characteristics for the exponential Rosenbrock-type method.

5.2. **Numerical Testing of Method Order.** By running the exponential Rosenbrock-type solver on a modified version of the decay to a circle system, I showed numerically that the average distance from the decayed solution is $O(1/\lambda)$. Here, the parameter c changes the fast dynamics so that they do not also correspond to rotation about the circle. Now the dynamics of the system push the solution curve toward an elliptical shape.

$$\begin{cases} \dot{x} = -y - \lambda x(x^2+y^2-1) \\ \dot{y} = \ cx - \lambda y(x^2+y^2-1) \end{cases}$$

Here, the stable manifold is the unit circle, $x^2+y^2=1$. The leading order source of $\hat{P}_{\text{fast}}\mathbf{f}$ is the cx term, but this behavior is not large in λ. Hence, as λ increases, the solution conforms more to a circle, and average distance from the circle decreases. In Figure 8, $1/\lambda$ is plotted on a logarithmic scale against average distance from the unit circle, for the cases where $c = 2$ and $c = 4$. As expected, both cases are linear with a positive slope of one. The coefficient on $1/\lambda$ is slightly higher for $c = 4$ than for $c = 2$, but both cases have an average distance of $\mathrm{O}(1/\lambda)$

Comparing two versions of the method, with one step of h and two steps of $h/2$ shows how the method behaves numerically. In Figure 9, a single iteration of $|\mathbf{y} - \bar{\mathbf{y}}|$ is plotted against step size, for multiple values of λ. Note that for small values of λ, the method performs as a second order method, while for larger values of λ, the method performs only as a first order method.

FIGURE 8. $1/\lambda$ vs. Average distance from unit circle, for multiple values of c

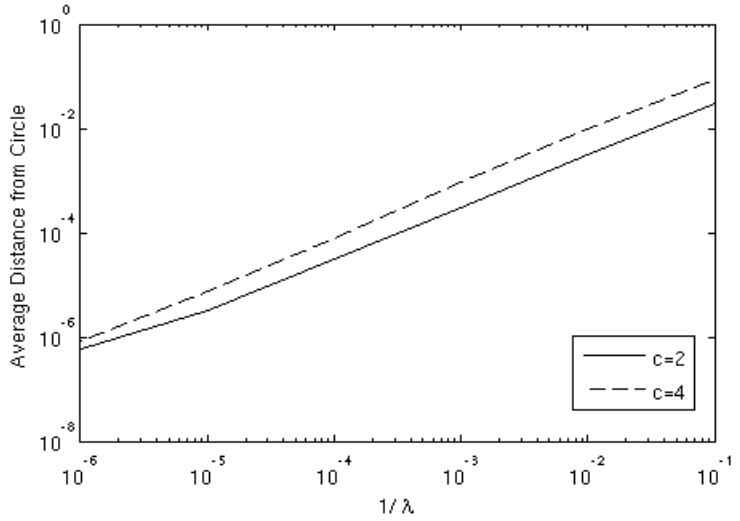

FIGURE 9. The absolute value of the difference $\mathbf{y}$ and $\bar{\mathbf{y}}$, obtained by one step of size h, and two steps of size $h/2$, respectively. Dotted lines indicate slopes of h, h^2, h^3.

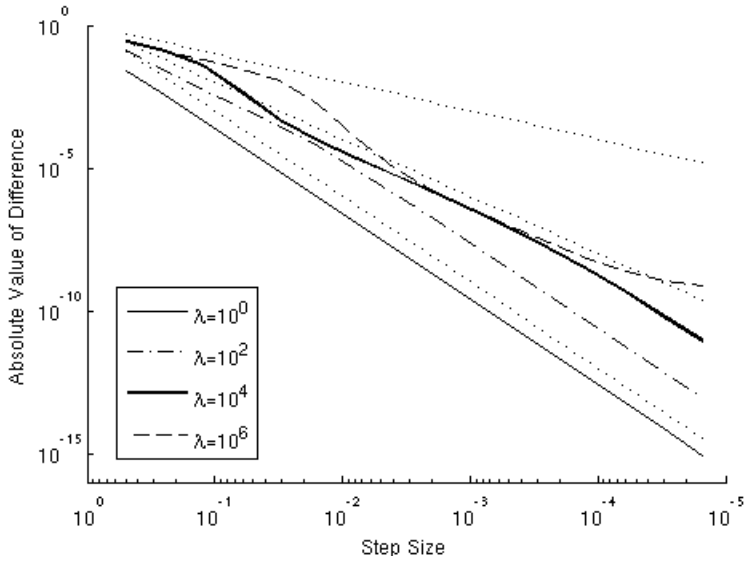

6. CONCLUDING REMARKS

Using estimation style analysis and numerical experimentation, I have shown that after the decay of the rapid modes, the solution curve is O(h) from the surface of slow dynamics. I have also shown that in the stiff limit, the exponential Rosenbrock-type method suffers an order reduction to first order. This order reduction in the limit is typical behavior for an ODE solver.

The method exhibits stiffness characteristics, but more numerical experimentation of the stiff limit is recommended. Ideally, this experimentation would be as independent of the choice of step size as possible. The code used for this research chooses step size based on the tolerance threshold; hence, step size is implicitly determined by the tolerance. In addition, more investigation into the size of the nonlinear terms from the expansion of $\tilde{\mathcal{F}}$ is recommended, to determine whether the nonlinear terms are indeed small enough to neglect.

ACKNOWLEDGEMENTS

I would like to thank Dr. Misha Stepanov for continuous support and encouragement throughout the semester.

REFERENCES

1. Uri M. Ascher and Linda R. Petzold, *Computer methods for ordinary differential equations and differential-algebraic equations*, 1st ed., Society for Industrial and Applied Mathematics, Philadelphia, PA, USA, 1998.
2. Peter N. Brown, Alan C. Hindmarsh, and Homer F. Walker, *Experiments with quasi-newton methods in solving stiff ode systems*, SIAM J. Sci. Stat. Comput. **6** (1985), no. 2, 297–313.
3. W. H. Enright, T. E. Hull, and B. Lindberg, *Comparing numerical methods for stiff systems of o.d.e:s*, BIT Numerical Mathematics **15** (1975), 10–48, 10.1007/BF01932994.
4. M. Hochbruck, A. Ostermann, and J. Schweitzer, *Exponential rosenbrock-type methods*, J. Numer. Anal. **47** (2009), 786–803.